Modelling the impact of the Omicron BA.5 subvariant in New Zealand

Audrey Lustig, Giorgia Vattiato, Oliver Maclaren,
Leighton M. Watson, Samik Datta, Michael J. Plank

Abstract

New Zealand experienced a wave of the Omicron variant of SARS-CoV-2 in early 2022, which occurred against a backdrop of high two-dose vaccination rates, ongoing rollout of boosters and paediatric doses, and negligible levels of prior infection. New Omicron subvariants have subsequently emerged with a significant growth advantage over the previously dominant BA.2. We investigated a mathematical model that included waning of vaccine-derived and infection-derived immunity, as well as the impact of the BA.5 subvariant which began spreading in New Zealand in May 2022. The model was used to provide scenarios to the New Zealand Government with differing levels of BA.5 growth advantage, helping to inform policy response and healthcare system preparedness during the winter period. In all scenarios investigated, the projected peak in new infections during the BA.5 wave was smaller than in the first Omicron wave in March 2022. However, results indicated that the peak hospital occupancy was likely to be higher than in March 2022, primarily due to a shift in the age distribution of infections to older groups. We compare model results to subsequent epidemiological data and show that the model provided a good projection of cases, hospitalisations and deaths during the BA.5 wave.

Introduction

The B.1.1.529 (Omicron) variant of SARS-CoV-2 was designated a variant of concern by the World Health Organisation on 26 November 2021 (World Health Organisation, 2021) subsequent to a rapid growth in cases of Covid-19 in southern Africa (Viana et al., 2022). Following leakage of imported cases from managed isolation facilities in Jaunary 2022 (Douglas et al., 2022), New Zealand experienced a large Omicron wave with around 220 confirmed cases per 1,000 people between 1 February and 31 May 2022. This wave was dominated by the BA.2 subvariant, which accounted for an estimated 84% of cases, with BA.1 accounting for the remaining 16%. In the week ending 29 May 2022, over 95% of sequenced new community cases were BA.2 (ESR, 2022a).

Prior to the arrival of Omicron, the total number of confirmed cases of Covid-19 in New Zealand was only around 0.3% of the population due to a combination of border restrictions, vaccination, and strong public health measures (Baker et al., 2020). This meant that the level of immunity from prior infection at the start of the wave was negligible. By 1 February 2022, 77% of the population (90% of those aged over 12 years) had received at least two vaccine doses and 27% of the population (35% of those aged over 18 years) had received a third dose. By 1 April 2022, third dose coverage had increased to 51% of the population (66% of those aged over 18 years). In addition, those aged 5 to 11 years became eligible for vaccination on 17 January 2022 and by 1 April, 54% of this age group had received at least one dose and 17% had received two doses. The Pfizer/BioNTech BNT162b2 vaccine was the main vaccine in use and accounted for the vast majority of all doses administered.

Public health measures to control the spread of the virus were applied as part of New Zealand's Covid-19 Protection Framework (New Zealand Government, 2021). The country was moved to the Red setting of the framework on 23 January 2022, which included widespread mask mandates, gathering size limits, vaccine pass requirements for many businesses, and encouraged working from home. These restrictions were relaxed in stages with outdoor gathering restrictions removed and indoor gathering size limits increased from 100 to 200 on 25 March 2022. Vaccine pass requirements were removed on 4 April. The country was moved to the Orange setting on 13 April 2022, meaning that all gathering restrictions were lifted and masks were encouraged but no longer mandatory in schools. During this

period, isolation requirements were also progressively reduced from 14 days to 7 days and quarantine requirements were narrowed to just household contacts.

The BA.5 subvariant was first detected in South Africa in February 2022 (Tegally et al., 2022) and is closely related to BA.2. It carries distinct mutations in the spike protein, two of which are associated with higher transmissibility and immune evasion (Cao et al., 2022; Tuekprakhon et al., 2022). BA.5 has driven waves of Covid-19 in multiple countries (UKHSA, 2022). The rise in BA.5 stems at least in part from its ability to infect people who were immune to earlier variants, but so far there is no indication the variant causes more severe disease. BA.5 was first detected in the New Zealand community in April 2022, and cases have been appearing consistently since May. It quickly rose to 32% of sequenced community cases by the beginning of July and became the dominant variant in early July 2022 (ESR, 2022a).

We have previously modelled the spread and impact of the Omicron variant of SARS-CoV-2 in New Zealand using an age-structured stochastic model (Vattiato et al., 2022b). This model included the effects of age-specific vaccination rates, different vaccine effectiveness against different clinical endpoints, and waning of vaccine-derived immunity. The model results were reasonably consistent with the observed numbers of cases, hospitalisations and deaths during the first wave up to early April 2022. Due to the high prevalence of cases in the community during 2022, in this work we switch from a stochastic to deterministic model, which significantly increases computational efficiency with negligible impact on the overall epidemic dynamics.

Here, we generalise this model to include waning of infection-derived immunity, meaning that people can can be re-infected with the virus for a second time. We also incorporate a simplified model for the effects of a new variant with different transmissibility and immune escape characteristics becoming dominant. We calibrate model parameters for the new variant using estimates of the growth advantage of BA.5 relative to BA.2 from data on whole genome sequencing of community cases (ESR, 2022b). We fit the model to New Zealand epidemiological data up to early July 2022, and use the model to estimate the future impact of the BA.5 subvariant under different levels of immune escape. These results were used to inform New Zealand government policy and healthcare system preparedness in advance of and during the wave. Here, we compare the model projections with subsequent data on new

daily cases, hospital admissions and deaths.

Methods

The susceptible population is divided into n_A age groups and n_S susceptible compartments per age group, denoted S_{ik} for $i = 1, \ldots, n_A$ and $k = 1, \ldots, n_S$. The susceptible states represent different levels of vaccine-derived and infection-derived immunity (Figure 1). Each state k is associated with a set of immunity parameters e_{Ok} representing immunity against different outcomes O (see *Immunity model* section). Transmission between age groups is governed by a contact matrix (Prem et al., 2017; Vattiato et al., 2022b). See Supplementary Material Sec. 1.1 for details of the ordinary differential equations governing transmission dynamics. Matlab code to run the model and reproduce the results is available at https://github.com/michaelplanknz/modelling-ba5-in-nz.

The model structure is similar to that of the stochastic model of Vattiato et al. (2022b) but is generalised to include waning of infection-derived immunity and the effects of fourth and potentially subsequent doses of the vaccine. Using a deterministic model ignores stochastic fluctuations in daily infection rates, although this is likely to have a relatively small effect on epidemic dynamics during periods of relatively high prevalence. In addition, high levels of prior infection mean that transmission is primarily controlled by immunity, which creates negative feedback on stochastic deviations from a mean-field model. The waning model is similar to Keeling et al. (2021) but the inclusion of a series of post-recovery susceptible compartments means the model is not restricted to exponential waning curves and can capture differing dynamics of immunity against infection and immunity against severe disease.

Vaccination rates are based on the number of vaccine doses per day given to people in age group i at time t, plus estimated future uptake of fourth doses according to Ministry of Health projections (see Supplementary Figure 1). Case reporting, hospital admissions and discharges, and deaths are modelled via age-dependent rates of clinical disease, hospitalisation and fatality and probability of testing (see Supplementary Material Sec. 1.5 and Supplementary Tables 1–2).

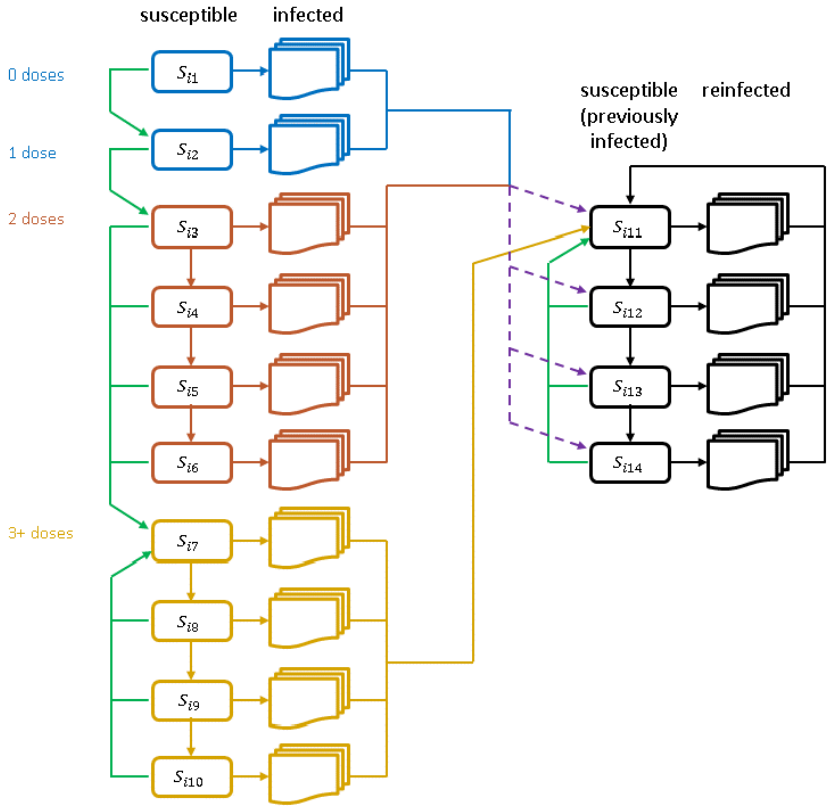

Figure 1: Schematic diagram of the model structure showing the 14 susceptible compartments for age group i, indexed as compartments S_{ik} for $k = 1, \ldots, 14$. Vertical downward arrows represent transition to a susceptible compartment with lower immunity as a result of waning immunity. Green arrows represent transition to a susceptible compartment with higher immunity as a result of vaccination. Horizontal arrows represent infection, which initiates transition through a series of disease states ending in recovery. Following recovery from first infection, individuals who have had at least three vaccine doses (yellow) transition to the highest immunity post-infection compartment $S_{i,11}$; individuals who have had fewer than three vaccine doses (blue and red) transition to a mixture of compartments $S_{i,11}$ to $S_{i,14}$ (dashed purple arrows), representing lower post-infection immunity for these groups. Following recovery from a second or subsequent infection (black), all individuals transition to $S_{i,11}$ regardless of vaccination status.

Immunity model

The model includes parameters representing the level of immunity against infection ($e_{I,k}$), symptomatic disease ($e_{S,k}$), transmission ($e_{T,k}$), hospitalisation ($e_{H,k}$) and death ($e_{F,k}$) for people in susceptible compartment k. In principle, this means there are a total of up to 70 immunity parameters in the model (14 susceptible compartments times 5 endpoints). To provide a parsimonious parameterisation, we use the model of Khoury et al. (2021) and Cromer et al. (2022b) for the relationship between level of immunity and neutralising antibody titre. This approach to parameterising models has also been used for other groups carrying out epidemiological modelling for policy advice (e.g. Barnard et al., 2021). The antibody titre is assumed to be a correlate of protection and a given titre is generally more protective against more serious clinical endpoints, in line with the findings of Cromer et al. (2022a). This framework enables laboratory data from neutralisation experiments to be combined with population-level data to produce estimates of time-varying immunity from different sources, to different endpoints, resulting from infection with different variants of SARS-CoV-2 (Golding and Lydeamore, 2022).

We use the estimates of Golding and Lydeamore (2022) to determine the initial log antibody titre $n_{i,0}$ associated with each source of immunity i in our model (2 or 3 vaccine doses with or without prior infection). To model waning immunity, we assume that the log antibody titre decreases by a fixed amount for each successive susceptible compartment in the same category (i.e. through compartments $k = 3, \ldots, 6$, $k = 7, \ldots, 10$ and $k = 11, \ldots, 14$). We then map the log antibody titre n_k for compartment k to immunity e_{Ok} against outcome O via a logistic function with an outcome-specific midpoint parameter $n_{O,50}$ (Khoury et al., 2021):

$$e_{Ok} = \frac{1}{1 + e^{-\kappa(n_k - n_{O,50})}}. \tag{1}$$

This framework means the immunity model can be parameterised with one parameter $n_{i,0}$ for each source of immunity i, one parameter for each outcome O and two additional independent parameters: the logistic slope κ; and the transition rate r_w between successive susceptible compartments, which represents the speed of waning (see Supplementary Table 3).

For the post-infection susceptible states, we do not have separate sets of susceptible compartments for people with different vaccination status. Instead, we model vaccination-dependent

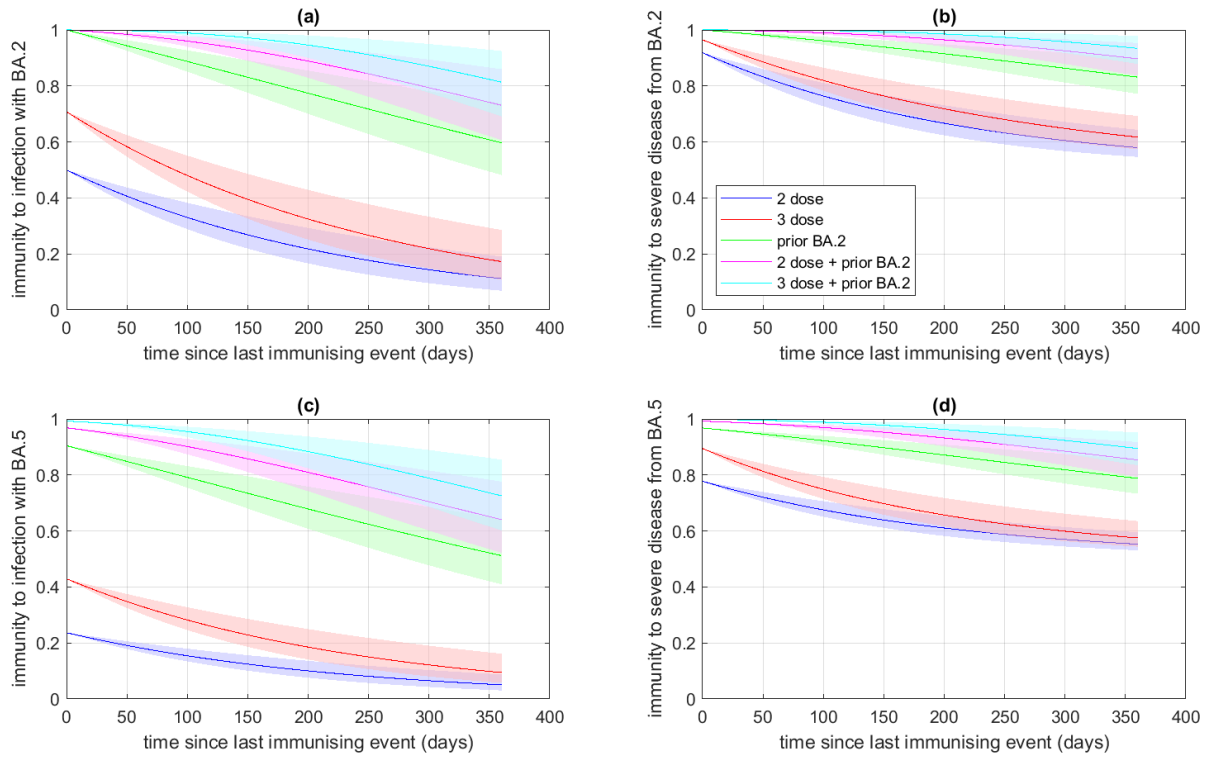

Figure 2: Average immunity under assumed parameter priors against: (a) infection with BA.2; (b) severe disease or death from BA.2; (c) infection with BA.5; (d) severe disease or death from BA.5 as a function of time since most recent immunising event. Graphs show immunity following 2 doses (blue), 3 doses (red), 0/1 doses and prior infection with BA.2 (yellow), 2 doses and prior infection with BA.2 (purple) and 3 doses and prior infection with BA.2 (green). Immunity from two or more prior infections also follows the green trajectory, regardless of vaccination status. Immunity against BA.5 derived from prior infection with BA.5 is assumed to follow the same curves as for immunity against BA.2 derived from prior infection with BA.2. Curves are the median and shaded areas are the 5th and 95th percentiles of 500 random draws from the prior.

levels of post-infection immunity by moving people to different susceptible compartments dependent on their vaccination status. Following recovery from a first infection, people who have had 3 doses of the vaccine all move initially to the highest immunity compartment $k = 11$. People who have had fewer than 3 doses of the vaccine move to the lower-immunity compartments $k = 12, 13, 14$ in specified proportions (dashed purple arrows in Fig. 1, see Supplementary Material Sec. 1.4). We assume that, following recovery from a second or subsequent infection, everyone moves to the highest immunity compartment $k = 11$ regardless of vaccination status. We assume that a fourth dose of the vaccine prior to infection restores people to the same immunity level (susceptible compartment $k = 7$) as immediately after the third dose, and that any dose of the vaccine after recovery from infection moves people to the highest immunity level (susceptible compartment $k = 11$).

For simplicity, we set $e_{Tk} = 0$ and $e_{Sk} = e_{Ik}$, i.e. we assume that immunity reduces the risk of infection but, conditional on infection, does not change the likelihood of symptomatic disease or transmission. We also assume that immunity against hospitalisation and death never wane below $e_{\text{sev,min}} = 0.5$. This models a more durable component of the immune response, for example cellular immunity as opposed to neutralising antibodies, that maintains immunity against severe disease at some minimum long-term level. For the initial log titre following infection, we use somewhat higher values than those estimated by Golding and Lydeamore (2022) (see Supplementary Table 3). This is partly due to recent epidemiological studies suggesting that prior infection with BA.1/BA.2 provides relatively strong immunity against reinfection at least for several months (Altarawneh et al., 2022; Hansen et al., 2022; Malato et al., 2022), and partly due to empirical observations that the proportion of new cases in New Zealand that were potential reinfections (had a previously reported positive test result at least 28 days prior) was relatively low (below 4% up to the end of June 2022 – see Results). The average immunity from different sources against infection and against severe disease under assumed priors are shown in Figure 2.

Variant model

To model the effect of a new variant of concern (VOC), we use a simplified approach that can capture potential changes in intrinsic transmissibility and/or immune escape. This does not encompass the full dynamics of two or more variants spreading simultaneously with

partial cross-immunity (Kucharski et al., 2016), but captures the key effects by changing relevant model parameters around a specified time point t_{VOC} when the new variant becomes dominant. For simplicity, we assume that all infections prior to t_{VOC} are the resident variant (BA.2) and all infections after t_{VOC} are the new variant (BA.5).

A variant that has different intrinsic transmissibility can be modelled by a change in the parameter $R_{EI}(t)$ at $t = t_{VOC}$. A variant that evades immunity can be modelled by reducing the initial antibody titre levels $e_{2d,0}$ and $e_{3d,0}$ for vaccinated but not previously infected states at $t = t_{VOC}$ (Khoury et al., 2021). This is equivalent to a reduction in vaccine effectiveness. We assume that BA.5 has the same intrinsic transmissibility as BA.2, but there is a 2.5-fold drop in antibody titre against BA.5 relative to BA.2, which is consistent with lab studies on neutralisation (Khan et al., 2022; Hachmann et al., 2022).

Reducing the initial antibody titre for previously infected states ($k = 11, \ldots, 14$) would result in a permanent reduction in infected-induced immunity, including against future reinfection with the same variant. To avoid this, we instead model reduction in infection-derived antibody titre to the new variant by moving individuals in the previously infected states ($k = 11$, 12 or 13) at $t = t_{VOC}$ to a lower immunity state ($k = 12$, 13 or 14). This means that a reduction in average titre is applied to people infected before $t = t_{VOC}$ (assumed to be infection with the resident variant), but people infected after $t = t_{VOC}$ (assumed to be infection with the new variant) start with the same initial antibody titre following recovery as before the new variant arrived. Thus, the model assumes an equally high level of homologous immunity against reinfection with the same variant (whether resident→resident or VOC→VOC) but a relatively lower level of cross-reactive immunity to the new variant (resident→VOC).

The magnitude of the drop in infection-derived immunity to the new variant is determined by a dimensionless parameter r_{VOC} (see Supplementary Material Sec. 1.4). In practice, the value of r_{VOC} was chosen such that the change in epidemic growth rate at time $t = t_{VOC}$ corresponds to the empirically observed growth advantage of the new variant relative to the resident variant. The growth rate of BA.5 relative to BA.2 in genomically sequenced New Zealand community cases reported up to 21 June 2022 (ESR, 2022b) was estimated to be 0.10 day^{-1} (95% CI 0.073–0.128 day^{-1}) via multinomial regression (see Supplementary Figure 2). This is consistent with international estimates of the growth advantage of BA.5

over BA.2 which are generally in range 0.07 to 0.14 day^{-1} (Tegally et al., 2022; UKHSA, 2022). Values of $r_{\mathrm{VOC}} = 0.39 \pm 0.2$ were found to produce an increase in epidemic growth rate consistent with these estimates. Due to a lack of evidence to the contrary, we assumed that there is no change in disease severity for BA.5 compared to BA.2.

Parameter inference and model fitting

We take a simple approximate Bayesian computation (ABC rejection) approach to fit the model to data. For each combination of parameter values drawn from the prior, we solve the model and calculate the error function $d(x, y)$ where x is the time series of model outputs for a specified variable and y is the corresponding data time series. The 1% of model simulations with the smallest values of the error function are retained. We fit the following model outputs: (1) new daily cases; (2) proportion of new cases in over 60s; (3) new daily hospital admissions; (4) daily deaths; (5) new weekly infections in routinely tested border workers (see Supplementary Material Sec. 1.5 for definitions).

Prior distributions for fitted parameters are shown in Supplementary Tables 1–3. Generally, these are relatively informative priors that represent modest uncertainty in parameter estimates. These include changes in the value of the reproduction number excluding immunity $R_{EI}(t)$ and contact matrix M during specified time windows to model changes in mixing rates as a result of public health interventions or voluntary behavioural change. The value of $R_{EI}(t)$ was assumed to increase linearly from $R_{EI,1}$ to $R_{EI,2}$ starting around 10 March 2022 and over a window of 30–50 days (see Supplementary Table 1). The contact matrix M was initially set to the matrix in Vattiato et al. (2022a), denoted M_0, to provide a reasonable match with the observed age distribution of cases in the first part of the simulated time period. The contact matrix M was assumed to change to a modified matrix $(1-\alpha_M)M_0+\alpha_M M_1$, where M_1 is the matrix estimated from pre-pandemic data (Prem et al., 2017; Steyn et al., 2022) and $\alpha_M \in [0, 1]$ is fitted to data. The change in contact matrix was assumed to occur linearly over a 70–90 day time windows starting at the same time as the change in $R_{EI}(t)$ (see Supplementary Table 1). These are ad hoc model adjustments which were observed to provide a reasonable fit to data and reflect plausible behavioural changes during the simulated time period.

Results

Results were fitted to data available as at 7 July 2022 on new daily cases, hospitalisations and deaths, the proportion of new cases in over-60-year-olds, and new weekly infections in a cohort of routinely tested border workers. Note that hospitalisations exclude those who are not being treated primarily for Covid-19 and deaths exclude those where the cause of death is classified as unrelated to Covid-19 by the Ministry of Health. To allow for reporting lags, the most recent 40 days of admissions data (admissions after 28 May 2022) and 10 days of deaths data (deaths after 27 June 2022) were excluded. We then compare model projections to subsequent data, available as at 22 September 2022.

Figure 3 shows model results for the baseline scenario (in which BA.5 has a growth rate of 0.09 per day relative to BA.2) and assuming that contact rates and government policy do not change in response to the wave. The growth advantage of BA.5 was estimated from data on sequenced community cases up to 21 June 2022 (ESR, 2022b) (see Methods). The model provides a reasonably good fit to the historic time series (purple curves and points in Figure 3) from the start of the first Omicron wave in February 2022 through to June 2022. The relatively long tail and flat plateau after the peak of the first Omicron wave in March 2022 can be explained by a gradual increase in the reproduction number excluding immunity $R_{EI}(t)$ in the model (see Figure 4) and relaxation of the contact matrix describing mixing between age groups towards pre-pandemic patterns. This can be interpreted as a gradual relaxation of public health measures (e.g. shortening of isolation period, narrowing definition of close contact, removal of gathering size limits and mask mandates in schools) and of voluntary risk-reduction behaviours between March and May 2022. A gradual increase in $R_{EI}(t)$ over a period of time rather than step increases on dates associated with specific policy changes is consistent with observations from the relaxation of public health restrictions in England in 2021 (Keeling et al., 2022).

Comparing with subsequently available data (green curves and points in Fig. 3), the peak in daily cases was slightly lower and occurred slightly earlier than the model predicted, although the trajectory remained within the 50% credible interval (CrI) of the model until after the peak, and within the 90% CrI (Fig. 3b) for the whole period. The peak in new daily hospital admissions (Fig. 3c) and hospital occupancy (Fig. 3g) were very close to model predictions.

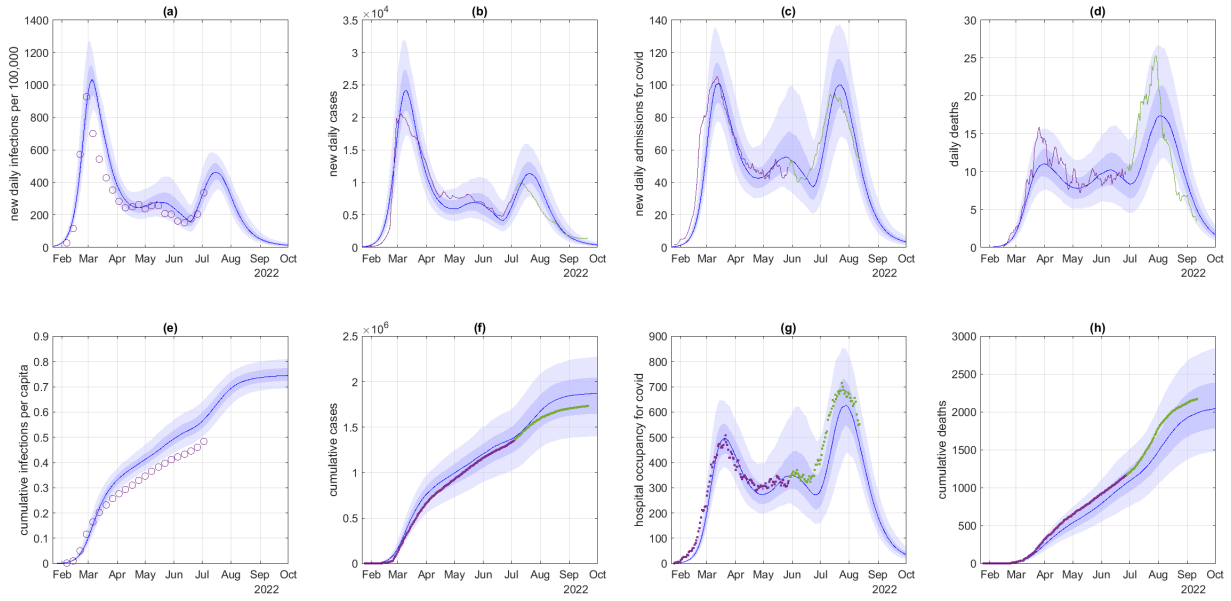

Figure 3: Results for the baseline scenario with no reduction in transmission: (a) daily infections per 100,000 people, (b) daily reported cases, (c) new daily hospital admissions for Covid-19, (d) daily Covid-19 deaths, (e) cumulative infections, (f) cumulative cases, (g) number of people receiving hospital treatment for Covid-19, (h) cumulative Covid-19 deaths. Blue curves show the median of 500 model simulations and shaded bands show the 5th, 25th, 75th and 95th percentiles. Purple curves/points show data available at 7 July 2022 that was used to fit the model; green curves/points show subsequent validation data. Data shown in (b)–(d) is a 7-day rolling average. Data for new daily infections per 100,000 in (a) show the rate of cases detected in a routinely tested cohort of border workers. Reported cases are lower than total infections due to under-reporting. The most recent 10 days of deaths data and 40 days of admissions data are excluded due to reporting lags. Note: hospital occupancy in (g) is lower then number of Covid-19 cases in hospital as reported in the Ministry of Health's daily updates, which includes some patients who are not being treated for Covid-19.

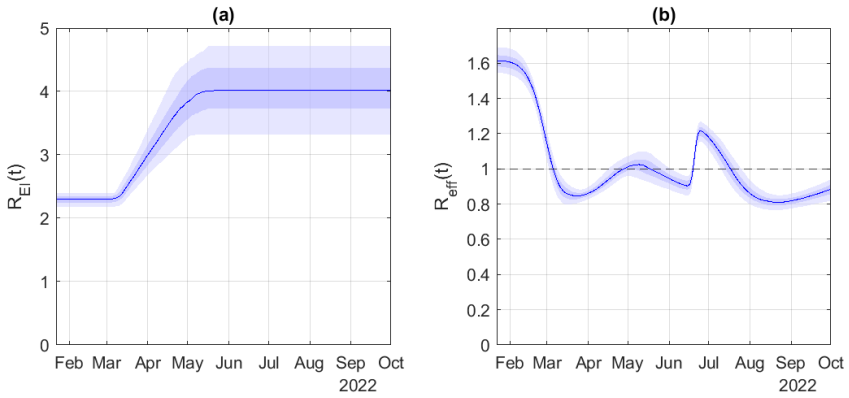

Figure 4: (a) Reproduction number excluding immunity $R_{EI}(t)$; and (b) effective time-varying reproduction number $R_{eff}(t)$. Blue curves show the median of 500 model simulations and shaded bands show the 5th, 25th, 75th and 95th percentiles. $R_{EI}(t)$ represents the potential spread rate in a fully susceptible population and changes in $R_{EI}(t)$ represent changes in contacts between individuals, as a result of changing public health measures and/or voluntary behaviour. $R_{eff}(t)$ represents the instantaneous reproduction number at time t including the effects of immunity. When $R_{eff}(t) > 1$ the number of new infections is increasing with time and when $R_{eff}(t) < 1$ the number of new infections is decreasing with time.

The model underestimated the number of Covid-19 deaths, although again the trajectory for daily deaths was within the 90% CrI of the model (Fig. 3d) and cumulative deaths were at the upper end of the 50% CrI (Fig. 3h). Notably, as predicted by the model, hospital occupancy and deaths were significantly higher in the July BA.5 wave than in the March BA.1/2 wave. Although new hospital admissions peaked at a similar level of around 100 per day in both waves, hospital occupancy peaked at around 500 in March and around 700 in July 2022. This is largely due to the fact that average length of hospital stay increases with age (see Supplementary Table 2). Similarly, deaths attributed to Covid-19 peaked at a seven-day rolling average of around 15 per day in March and 25 per day in July 2022. Scenarios where BA.5 has a smaller or larger growth advantage are shown in Supplementary Figures 7 and 8 respectively.

Stratifying cases, hospital admissions and deaths by 10-year age groups (Fig. 5) shows that the model provides a reasonable although imperfect representation of the age gradients in risk of infection and severe disease, and how these have changed over time. The first Omicron wave in March 2022 was dominated by younger age groups, particularly 10 to 30-year-olds. However, the age breakdown of cases has steadily shifted into older age groups over time (see Supplementary Figure 5) and the second wave (BA.5) was larger than the first wave (BA.2) in over 60-year-olds. The model captures this shift, although it underestimated the size of the BA.5 peak in over-70-year-olds, which is likely to be a key driver of the high number of deaths relative to the number of cases. The fact that the model groups everyone aged over 75 years into a single age band may also be contributing to systematically underestimating severe health outcomes as these will be sensitive to the age distribution of cases within this group. The model tends to underestimate hospital admissions and deaths in under 30-year-olds and overestimate them in 50-70-year-olds; this is likely a consequence of a slight misspecification in the assumed shape of the infection hospitalisation ratio and infection fatality ratio (Herrera-Esposito and de Los Campos, 2022) - see Supplementary Figure 6. It may also be affected by the fact that cause-of-death data is still not available for approximately 10% of deaths that have occurred within 28 days of a positive Covid-19 test.

Figure 6 shows the proportion of new reported cases that are reinfections. In the model, the true proportion of cases that are reinfections (blue curves in Fig. 6) increased from around 5% prior at the start of June 2022 to around 30% by October 2022. The rapid increase in

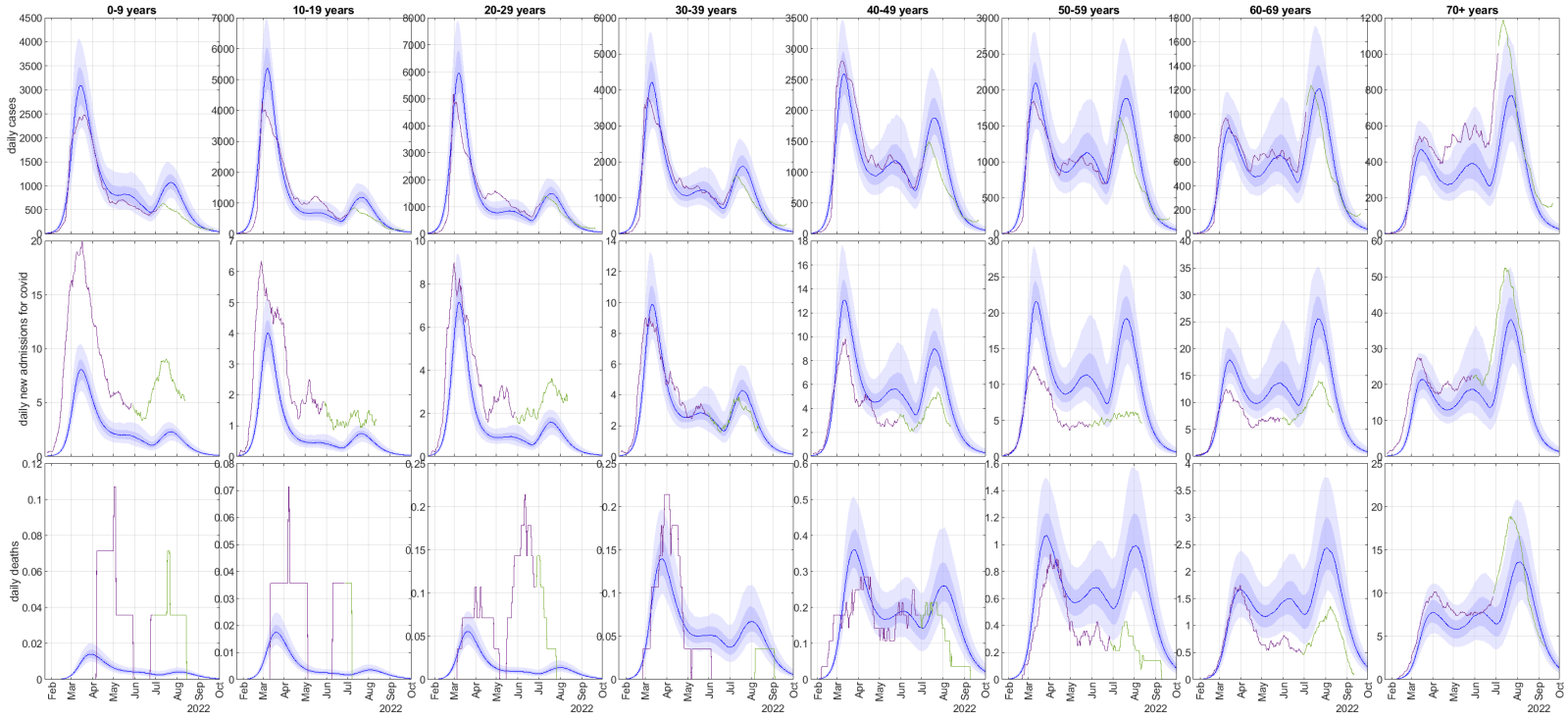

Figure 5: Age-stratified results for the baseline scenario showing new daily cases, new daily hospital admissions and daily deaths. Blue curve shows the median of 500 model simulations and shaded bands show the 5th, 25th, 75th and 95th percentiles. Purple curves show data available at 7 July 2022; green curves show subsequent validation data. Data is shown as a rolling average over 7 days for cases, 14 days for admissions and 28 days for deaths. Note different y-axis scales in different plots.

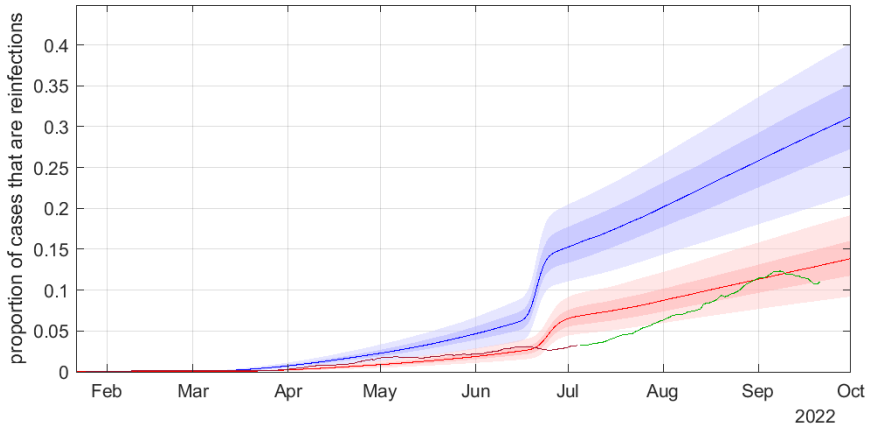

Figure 6: Proportion of reported cases that are reinfections. Model results show the true proportion of new reported cases that are reinfections (blue curve and bands) and the proportion adjusted for under-ascertainment of the first infection (red curve and bands). Curves shows the median of 500 model simulations and shaded bands show the 5th, 25th, 75th and 95th percentiles. Data available on 7 July 2022 (purple curve) and after 7 July 2022 (green curve) show the 7-day rolling average number of new cases that have previously reported a positive SARS-CoV-2 test at least 28 days prior as a fraction of the 7-day rolling average of total new cases.

reinfections seen in late June 2022 in the model is due to the greater ability of the BA.5 subvariant to evade immunity from prior infection with BA.2. In reality, cases can only be classified as reinfections if both the first and second infection were confirmed and reported to the Ministry of Health. Adjusting for underascertainment of first infections according to the age-specific case ascertainment ratio in the model results in a lower estimated reinfection rate (red curves in Fig. 6). This agrees more closely with empirical observations, although the increase in reinfections occurred more gradually than the model predicted. This comparison is subject to several biases and should be viewed as approximate. For example, the adjustment of model output for underascertainment of first infections assumes that reporting of first and subsequent reinfections occur independently with the same probability. Similarly, data on reinfections could be biased upwards if there is individual-level heterogeneity in propensity to report an infection that persists through time, or biased downwards if people are less likely to test or report a second infection. It is also possible that in some cases the second positive test result could represent a chronic infection rather than a reinfection.

Discussion

We have presented a mathematical model for SARS-CoV-2 in New Zealand since the arrival of Omicron in January 2022 that was used to estimate the impact of the recent BA.5 wave. Strengths of the model include that it is fitted to five separate data series spanning a 5-month period – daily Covid-19 cases, hospital admissions and deaths, proportion of new cases in over-60-year-olds, and new weekly infections in a routinely tested cohort. The model strikes a balance between including sufficient complexity to capture the most important mechanisms affecting epidemic dynamics and explaining historical patterns, while remaining simple enough that results that can be explained and understood with reference to particular assumptions. This is important for communicating results to policymakers and practitioners and avoids having a large number of unknown parameters and/or overfitting. Our results showed that the model made reasonable projections of the BA.5 wave in July and August 2022.

However, the model has a number of limitations and sources of uncertainty. We have fitted the model to data using relatively informative priors for selected parameters. This provides a range of parameter combinations which are consistent with empirical data, but it cannot rule out that other parameter combinations or other sets of model assumptions could provide an equally good fit. This means that the uncertainty bands plotted in model results likely underestimate true uncertainty, especially when projecting model dynamics a long way into the future.

Reported cases are likely to be a significant underestimate of total infections, and the number of people infected with Omicron to date is unknown. Although we have used data from a routinely tested cohort of border workers, this cohort may not be representative of the population. This means the extent of infection-derived immunity in the population is uncertain. This uncertainty could be overcome in future by regular testing of a representative sample for SARS-CoV-2 (Riley et al., 2020; Pouwels et al., 2021).

Unlike previous waves of SARS-CoV-2 in New Zealand, immunity is now the single biggest factor affecting transmission dynamics. The immune landscape has become more complex over time, with various combinations of immunity derived from vaccination and prior infection with different subvariants at different time points. The model necessarily made

simplifying assumptions about the nature of the immunity landscape and it is possible that results are sensitive to these assumptions.

Estimates for the level of immune escape of BA.5 are subject to uncertainty and this was a key factor determining the size of the wave. We estimated the growth advantage of BA.5 relative to BA.2 from data on sequenced community cases reported up to 21 June 2022 (ESR, 2022b). Although this gave an estimate which was consistent with international estimates (UKHSA, 2022), it should be remembered that sequenced cases are not necessarily representative of all cases and there is still a range of possible values for model parameters relating to the characteristics of BA.5. The effect of immune escape and reinfection on the risk of severe disease and death is also uncertain, and this could have affected the projected case hospitalisation ratio and case fatality ratio.

The extent, if any, of behavioural change in response to a SARS-CoV-2 wave is difficult to predict in advance. Although behavioural change is known to have had a significant effect on previous waves in New Zealand and internationally, it could not be assumed that the response would be comparable for the BA.5 wave or future waves. The model assumed that mixing within and between age groups could be reasonably approximated by an age-structured contact matrix. It is likely that population heterogeneity not accounted for in the model has a significant effect on the point at which new infections peak and start to decline. The size and timing of peaks are inherently uncertain because they are sensitive to variables and parameters that are not precisely known including those mentioned above.

We only modelled the impacts of the BA.5 wave at the aggregate national level. These results will mask significant regional and demographic variation. Some groups are likely to be disproportionately affected such as those working in public-facing roles and insecure employment, people in overcrowded or substandard housing, Māori and Pacific people (McLeod et al., 2020; Steyn et al., 2021), and people without good access to healthcare, testing, masks and vaccines (Whitehead et al., 2021).

Acknowledgements

The authors acknowledge the role of the New Zealand Ministry of Health, StatsNZ, and the Institute of Environmental Science and Research in supplying data in support of this work. The authors are grateful to Michael Bunce, Emily Harvey, August Hao, Nick Golding, James McCaw, Dion O'Neale, Gerry Ryan, Freya Shearer and David Welch for discussions about modelling immunity and the growth of BA.5, and to Nigel French, Markus Luczak-Roesch, Matt Parry, and the Covid-19 Modelling Government Steering Group for feedback on earlier versions of this report. This work was funded by the New Zealand Department of Prime Minister and Cabinet.

References

Altarawneh, H. N., Chemaitelly, H., Ayoub, H., Hasan, M. R., Coyle, P., YASSINE, H. M., Al Khatib, H. A., Benslimane, F., Al-Kanaani, Z., Al Kuwari, E., et al. (2022). Protection of SARS-CoV-2 natural infection against reinfection with the BA.4 or BA.5 Omicron subvariants. *medRxiv*, https://doi.org/10.1101/2022.07.11.22277448.

Baker, M. G., Wilson, N., and Anglemyer, A. (2020). Successful elimination of Covid-19 transmission in New Zealand. *New England Journal of Medicine*, 383(8):e56.

Barnard, R. C., Davies, N. G., Pearson, C. A., Jit, M., and Edmunds, W. J. (2021). Projected epidemiological consequences of the omicron sars-cov-2 variant in england, december 2021 to april 2022. *medRxiv*, https://doi.org/10.1101/2021.12.15.21267858.

Cao, Y., Yisimayi, A., Jian, F., Song, W., Xiao, T., Wang, L., Du, S., Wang, J., Li, Q., Chen, X., et al. (2022). BA.2.12. 1, BA.4 and BA.5 escape antibodies elicited by Omicron infection. *Nature*, https://doi.org/10.1038/s41586-022-04980-y.

Cromer, D., Steain, M., Reynaldi, A., Schlub, T. E., Sasson, S. C., Kent, S. J., Khoury, D. S., and Davenport, M. P. (2022a). Neutralising antibodies predict protection from severe COVID-19. *medRxiv*, https://doi.org/10.1101/2022.06.09.22275942.

Cromer, D., Steain, M., Reynaldi, A., Schlub, T. E., Wheatley, A. K., Juno, J. A., Kent, S. J., Triccas, J. A., Khoury, D. S., and Davenport, M. P. (2022b). Neutralising antibody

titres as predictors of protection against SARS-CoV-2 variants and the impact of boosting: a meta-analysis. *Lancet Microbe*, 3(1):e52–e61.

Douglas, J., Winter, D., Ren, X., McNeill, A., Bunce, M., French, N., Hadfield, J., de Ligt, J., Welch, D., and Geoghegan, J. L. (2022). Tracing the international arrivals of SARS-CoV-2 Omicron variants after Aotearoa New Zealand reopened its border. *medRxiv*, https://doi.org/10.1101/2022.07.12.22277518.

ESR (2022a). Genomics insights dashboard. https://esr2.cwp.govt.nz/our-expertise/covid-19-response/covid19-insights/genomics-insights-dashboard/. Accessed 2 July 2022.

ESR (2022b). Prevelence of SARS-CoV-2 variants of concern in Aoteoroa New Zealand. https://github.com/ESR-NZ/nz-sars-cov2-variants.

Golding, N. and Lydeamore, M. (2022). Analyses to predict the efficacy and waning of vaccines and previous infection against transmission and clinical outcomes of SARS-CoV-2 variants. https://github.com/goldingn/neuts2efficacy. Accessed 5 April 2022.

Hachmann, N. P., Miller, J., Collier, A.-r. Y., Ventura, J. D., Yu, J., Rowe, M., Bondzie, E. A., Powers, O., Surve, N., Hall, K., et al. (2022). Neutralization escape by SARS-CoV-2 Omicron subvariants BA.2.12.1, BA.4, and BA.5. *New England Journal of Medicine*, 387:86–88.

Hansen, C. H., Friis, N. U., Bager, P., Stegger, M., Fonager, J., Fomsgaard, A., Gram, M. A., Engbo Christiansen, L., Ethelberg, S., Legarth, R., et al. (2022). Risk of reinfection, vaccine protection, and severity of infection with the BA.5 Omicron subvariant: A Danish nationwide population-based study. *Available at SSRN*, https://dx.doi.org/10.2139/ssrn.4165630.

Herrera-Esposito, D. and de Los Campos, G. (2022). Age-specific rate of severe and critical SARS-CoV-2 infections estimated with multi-country seroprevalence studies. *BMC Infectious Diseases*, 22(1):1–14.

Keeling, M. J., Brooks-Pollock, E., Challen, R. J., Danon, L., Dyson, L., Gog, J. R., Guzman-Rincon, L., Hill, E. M., Pellis, L. M., Read, J. M., et al. (2021). Short-term Projections based on Early Omicron Variant Dynamics in England. *medRxiv*, https://doi.org/10.1101/2021.12.30.21268307.

Keeling, M. J., Dyson, L., Tildesley, M. J., Hill, E. M., and Moore, S. (2022). Comparison of the 2021 COVID-19 roadmap projections against public health data in England. *Nature Communications*, 13(1):1–19.

Khan, K., Karim, F., Ganga, Y., Bernstein, M., Jule, Z., Reedoy, K., Cele, S., Lustig, G., Amoako, D., Wolter, N., et al. (2022). Omicron sub-lineages BA.4/BA.5 escape BA.1 infection elicited neutralizing immunity. *medRxiv*, https://doi.org/10.1101/2022.04.29.22274477.

Khoury, D. S., Cromer, D., Reynaldi, A., Schlub, T. E., Wheatley, A. K., Juno, J. A., Subbarao, K., Kent, S. J., Triccas, J. A., and Davenport, M. P. (2021). Neutralizing antibody levels are highly predictive of immune protection from symptomatic SARS-CoV-2 infection. *Nature Medicine*, 27(7):1205–1211.

Kucharski, A. J., Andreasen, V., and Gog, J. R. (2016). Capturing the dynamics of pathogens with many strains. *Journal of Mathematical Biology*, 72(1):1–24.

Malato, J., Ribeiro, R. M., Leite, P. P., Casaca, P., Fernandes, E., Antunes, C., Fonseca, V. R., Gomes, M. C., and Graca, L. (2022). Risk of BA.5 infection among persons exposed to prior SARS-CoV-2 variants. *New England Journal of Medicine*, DOI: 10.1056/NEJMc2209479.

McLeod, M., Gurney, J., Harris, R., Cormack, D., and King, P. (2020). COVID-19: we must not forget about Indigenous health and equity. *Australian and New Zealand Journal of Public Health*.

New Zealand Government (2021). Covid-19 public health response (protection framework) order. New Zealand legislation 2021;(sl 2021/386). https://www.legislation.govt.nz/regulation/public/2021/0386/latest/LMS563461.html.

Pouwels, K. B., House, T., Pritchard, E., Robotham, J. V., Birrell, P. J., Gelman, A., Vihta, K.-D., Bowers, N., Boreham, I., Thomas, H., Lewis, J., Bell, I., Bell, J. I., Newton, J. N., Farrar, J., Diamond, I., Benton, P., Walker, A. S., and COVID-19 Infection Survey Team (2021). Community prevalence of SARS-CoV-2 in England from April to November, 2020: results from the ONS coronavirus infection survey. *Lancet Public Health*, 6(1):e30–e38.

Prem, K., Cook, A. R., and Jit, M. (2017). Projecting social contact matrices in 152 countries using contact surveys and demographic data. *PLoS Computational Biology*, 13(9):e1005697.

Riley, S., Atchison, C., Ashby, D., Donnelly, C. A., Barclay, W., Cooke, G. S., Ward, H., Darzi, A., Elliott, P., and REACT Study Group (2020). Real-time assessment of community transmission (REACT) of SARS-CoV-2 virus: study protocol. *Wellcome Open Research*, 5.

Steyn, N., Binny, R. N., Hannah, K., Hendy, S., James, A., Lustig, A., Ridings, K., Plank, M. J., and Sporle, A. (2021). Māori and Pacific people in New Zealand have higher risk of hospitalisation for COVID-19. *New Zealand Medical Journal*, 134:28–43.

Steyn, N., Plank, M. J., Binny, R. N., Hendy, S. C., Lustig, A., and Ridings, K. (2022). A COVID-19 vaccination model for Aotearoa New Zealand. *Scientific Reports*, 12(1):1–11.

Tegally, H., Moir, M., Everatt, J., Giovanetti, M., Scheepers, C., Wilkinson, E., Subramoney, K., Makatini, Z., Moyo, S., Amoako, D. G., et al. (2022). Emergence of SARS-CoV-2 Omicron lineages BA.4 and BA.5 in South Africa. *Nature Medicine*, https://doi.org/10.1038/s41591-022-01911-2.

Tuekprakhon, A., Huo, J., Nutalai, R., Dijokaite-Guraliuc, A., Zhou, D., Ginn, H. M., Selvaraj, M., Liu, C., Mentzer, A. J., Supasa, P., et al. (2022). Antibody escape of SARS-CoV-2 Omicron BA.4 and BA.5 from vaccine and BA.1 serum. *Cell*, 185:2422–2433.e13.

UKHSA (2022). SARS-CoV-2 variants of concern and variants under investigation in England. Technical briefing 42. https://www.gov.uk/government/publications/investigation-of-sars-cov-2-variants-technical-briefings.

Vattiato, G., Lustig, A., Maclaren, O., and Plank, M. J. (2022a). Modelling the dynamics of infection, waning of immunity and re-infection with the omicron variant of SARS-CoV-2 in Aotearoa New Zealand. *Covid-19 Modelling Aotearoa pre-print*, https://www.covid19modelling.ac.nz/waning-of-immunity-and-re-infection-with-omicron/.

Vattiato, G., Maclaren, O., Lustig, A., Binny, R. N., Hendy, S. C., and Plank, M. J. (2022b).

An assessment of the potential impact of the Omicron variant of SARS-CoV-2 in Aotearoa New Zealand. *Infectious Disease Modelling*, 7:94–105.

Viana, R., Moyo, S., Amoako, D. G., Tegally, H., Scheepers, C., Althaus, C. L., Anyaneji, U. J., Bester, P. A., Boni, M. F., Chand, M., et al. (2022). Rapid epidemic expansion of the SARS-CoV-2 Omicron variant in southern Africa. *Nature*, 603(7902):679–686.

Whitehead, J., Scott, N., Carr, P. A., and Lawrenson, R. (2021). Will access to Covid-19 vaccine in Aotearoa be equitable for priority populations? *International Journal of Epidemiology*, 50(Supplement_1):dyab168–708.

World Health Organisation (2021). Classification of Omicron (B.1.1.529): SARS-CoV-2 variant of concern. https://www.who.int/news/item/26-11-2021-classification-of-omicron-(b.1.1.529)-sars-cov-2-variant-of-concern.